

1 **Manuscript JVI02471-06: Revised January 31, 2007**

2

3

4 **Determination of the ex vivo rates of HIV-1 reverse transcription using novel**  
5 **strand-specific amplification (SSA) analysis**

6

7 David C. Thomas<sup>1,2</sup>, Yegor A. Voronin<sup>1,3</sup>, Galina N. Nikolenko<sup>1</sup>, Jianbo Chen<sup>4</sup>, Wei-  
8 Shau Hu<sup>4</sup> & Vinay K. Pathak<sup>1,\*</sup>

9

10 Running Title: Ex vivo kinetics of HIV-1 reverse transcription

11 <sup>1</sup>Viral Mutation Section, HIV Drug Resistance Program, National Cancer Institute at  
12 Frederick, Frederick, Maryland 21702. <sup>2</sup>Basic Research Program, SAIC-Frederick, Inc.,  
13 NCI-Frederick, Frederick, Maryland 21702. <sup>3</sup> Present address: Department of Human  
14 Biology, Fred Hutchinson Cancer Research Center, Seattle, Washington 98109, USA.

15 <sup>4</sup>Viral Recombination Section, HIV Drug Resistance Program, National Cancer Institute  
16 at Frederick, Frederick, Maryland 21702.

17

18 Abstract word count: 202

19 Text word count: 5,350

20

21 \*Corresponding author. Mailing address: Viral Mutation Section, HIV Drug Resistance  
22 Program, Center for Cancer Research, National Cancer Institute-Frederick, P. O. Box B,  
23 Room 334, Frederick Maryland, 21702. Phone: (301) 846-1710. Fax: (301) 846-6013.

24 E-mail: vpathak@ncifcrf.gov

25 **ABSTRACT**

26           **Replication of human immunodeficiency virus type 1 (HIV-1), like all**  
27 **organisms, involves synthesis of a minus-strand and a plus-strand of nucleic acid.**  
28 **Currently available PCR methods cannot distinguish between the two strands of**  
29 **nucleic acids. In order to carry out detailed analysis of HIV-1 reverse transcription**  
30 **from infected cells, we have developed a novel strand-specific amplification (SSA)**  
31 **assay using single-stranded padlock probes that are specifically hybridized to a**  
32 **target strand, ligated, and quantified for sensitive analysis of the kinetics of HIV-1**  
33 **reverse transcription in cells. Using SSA, we have determined for the first time the**  
34 ***ex vivo* rates of HIV-1 minus-strand DNA synthesis in 293T and human primary**  
35 **CD4<sup>+</sup> T cells (~68-70 nt/min). We also determined the rates of minus-strand DNA**  
36 **transfer (~4 min), plus-strand DNA transfer (~26 min) and initiation of plus-strand**  
37 **DNA synthesis (~9 min) in 293T cells. Additionally, our results indicate that plus-**  
38 **strand DNA synthesis is initiated at multiple sites and that several reverse**  
39 **transcriptase inhibitors influence the kinetics of minus-strand DNA synthesis**  
40 **differently, providing insights into their mechanism of inhibition. The SSA**  
41 **technology provides a novel approach to analyzing DNA replication processes and**  
42 **should facilitate development of new antiretroviral drugs that target specific steps in**  
43 **HIV-1 reverse transcription.**

## INTRODUCTION

44

45

46 Retroviral reverse transcriptases (RTs) convert a single-stranded viral RNA  
47 genome into a double-stranded DNA (4). Among the crucial events in the process of  
48 reverse transcription is initiation of minus-strand DNA synthesis to generate minus-strand  
49 strong-stop DNA, selective degradation of genomic RNA by RNase H, minus-strand  
50 DNA transfer, initiation of plus-strand DNA synthesis, formation of plus-strand strong-  
51 stop DNA, plus-strand DNA transfer and additional minus- and plus-strand DNA  
52 synthesis to complete the formation of viral DNA.

53 Several questions regarding the complex nature of HIV-1 reverse transcription in  
54 cells remain unanswered; these questions include the efficiency of DNA synthesis  
55 initiation and strand-transfer events, the rates of RNA- and DNA-dependent DNA  
56 synthesis, and preferential inhibition of minus- or plus-strand DNA synthesis by RT  
57 inhibitors. Studies using purified RT and template (5, 7, 9, 12, 18) as well as endogenous  
58 reverse transcription reactions using permeabilized virions (1, 19, 23) have provided  
59 insights into these questions. Additionally, recent application of real-time PCR  
60 technology (2, 24) has greatly facilitated the analysis of reverse transcription in cell-  
61 based assays; however, like all PCR methods, the real time PCR technique cannot  
62 distinguish between the two DNA strands and a system for quantitative strand-specific  
63 analysis of reverse transcription during the course of viral infection has not been  
64 available.

65 We have now developed a novel strand-specific amplification (SSA) assay for  
66 site-specific amplification and quantification of each strand during HIV-1 reverse

67 transcription and used it to measure the relative abundance of HIV-1 reverse transcription  
68 products generated at distinct steps over the time course of viral infection. These studies  
69 have allowed us to measure the kinetics of minus-strand DNA synthesis in 293T cells as  
70 well as human primary CD4<sup>+</sup> T cells, one of the target cells of HIV-1 infection. We have  
71 also measured the kinetics of plus-strand DNA synthesis and the efficiencies of minus-  
72 and plus-strand DNA initiation and transfer in 293T cells. Finally, we have used SSA to  
73 analyze the effects of RT inhibitors on minus- and plus-strand DNA synthesis, which  
74 provide insights into their mechanism of inhibition.

## 76 MATERIALS AND METHODS

78 **Plasmids and mutagenesis.** HIV-1-based retroviral vector pHDV-EGFP, which  
79 expresses HIV-1 Gag-Pol and the enhanced green fluorescent protein (EGFP) from the  
80 Nef open reading frame and does not express HIV-1 Env, was kindly provided by  
81 Derya Unutmaz (Vanderbilt University Medical Center, Nashville, TN) (22). pHCMV-G  
82 expresses vesicular stomatitis virus G envelope (VSV-G) (26). Site-directed mutagenesis  
83 of the cPPT in pHDV-EGFP was performed using the QuikChange XL Site-directed  
84 Mutagenesis Kit (Stratagene, Inc). The wild-type cPPT sequence (5'-  
85 AAAAGAAAAGGGGGG-3') was modified by introducing six silent mutations (5'-  
86 AAGCGCAAGGGCGGC-3'; the substitutions are underlined). A restriction fragment  
87 (*Sbf*I-*Sal*I) containing the cPPT was subcloned into the pHDV-EGFP plasmid to generate  
88 pHIV-GFP-cPPT<sup>-</sup> and sequenced to confirm the presence of the desired mutations and  
89 absence of undesired mutations.

90           **Preparation of virus particles.** For most experiments, virus was prepared from a  
91 293T-based cell line HIV-GFP2, which contains an undetermined number of integrated  
92 proviruses derived from pHDV-EGFP. To generate virus, HIV-GFP2 cells were plated at  
93  $2 \times 10^6$  cells per 100-mm-diameter dish and pretreated for two days before transfection  
94 with 1  $\mu$ M AZT for 10 h to prevent possible reinfection of transfected cells with  
95 produced virus. Calcium phosphate transfection (CalPhos transfection kit; Clontech) was  
96 performed using 4  $\mu$ g of VSV-G-expressing plasmid (26). After 7 h, DNA-containing  
97 transfection solution with 1  $\mu$ M AZT was removed by washing cells once with AZT-free  
98 medium and fresh medium was then added to the cells. The virus was collected 17 h later  
99 and concentrated 10-fold by ultracentrifugation at  $20,000 \times g$  for 1 h. After resuspension,  
100 the virus was treated with DNase I (30 units/ml, 10 mM final concentration of  $MgCl_2$ ) for  
101 1 h at room temperature, divided into 1-ml aliquots and frozen at  $-80^\circ C$ .

102           For some experiments, virus was produced following transient transfection of  
103 293T cells with pHDV-EGFP or pHIV-GFP-cPPT<sup>-</sup> and VSV-G-expressing plasmid,  
104 using the MBS Mammalian Transfection Kit (Stratagene). The treatment of virus  
105 produced from the transfected cells with DNase I (105 U/ml, 10 mM  $MgCl_2$ , 3 h at room  
106 temperature) resulted in very low background levels, indicating little contamination with  
107 transfected DNA.

108           **Time course for analyzing reverse transcription products in 293T cells.** In  
109 order to study the kinetics of HIV-1 reverse transcription, a time course of infection with  
110 HIV-1 HDV-EGFP virus was performed. For infection,  $2 \times 10^6$  or  $6 \times 10^5$  293T cells  
111 were plated per 100-mm- or 60-mm-diameter dish, respectively, the day before infection.  
112 A virus preparation concentrated 10-fold by centrifugation was diluted 20-fold in DMEM

113 medium. Two or 0.66 ml of diluted virus solution was used to infect 293T target cells  
114 plated on 100-mm- or 60-mm-diameter dish, respectively. After infection for 30 min, the  
115 virus was removed, cells were washed twice with phosphate-buffered saline to remove  
116 any residual virus and fresh medium was added to the plate. At the end of each time  
117 point, cells were washed twice with phosphate-buffered saline, resuspended in 2 ml of  
118 phosphate-buffered saline, pelleted and frozen until DNA isolation. In a typical time-  
119 course experiment, one plate of cells was collected at either 30-min or 1-h intervals up to  
120 6 h post-infection. Total cellular DNA was isolated using the QiaAmp DNA Blood Kit  
121 (Qiagen) and resuspended in 250-400  $\mu$ l of water. Real-time PCR or SSA analysis was  
122 performed four times for each primer-probe set using 4  $\mu$ l of this extracted DNA.

123 To monitor the efficiency of infection, the percentage of GFP-expressing cells  
124 was measured 48 h post-infection using flow cytometry (FACScan and Cell-Quest  
125 Software; Bectin Dickinson). In most experiments, 10-30% of the infected cells  
126 expressed GFP (multiplicity of infection <1).

127 To analyze the effects of RT inhibitors on reverse transcription, 293T cells were  
128 pretreated with the inhibitors for 24 h, and maintained in the presence of the drugs during  
129 and after the infection. The following concentrations of inhibitors were used: EFV, 9  
130 nM; ddI, 50  $\mu$ M; d4T, 4  $\mu$ M; AZT, 1  $\mu$ M. For each inhibitor, infection efficiencies were  
131 reduced 97-99% relative to a minus-inhibitor control infection, as determined by flow  
132 cytometry 36 h after infection.

133 **Time course for analyzing reverse transcription products in primary CD4<sup>+</sup> T**  
134 **cells.** Activated CD4<sup>+</sup> T cells were purified from human peripheral blood mononuclear  
135 cells (PBMCs) using the CD4 Positive Isolation Kit (DynaL Biotech) according to the

136 manufacturer's instructions. Cells were infected with HDV-EGFP virus by spinoculation  
137 as previously described; briefly, the cells were incubated for 2 h at  $1,200 \times g$  at  $10^{\circ}\text{C}$ ,  
138 followed by incubation at  $37^{\circ}\text{C}$  for 1 h (16). The cells were then washed four times to  
139 remove residual virus and placed back at  $37^{\circ}\text{C}$ . The cell samples for each time point  
140 during a time course were collected and processed as above for 293T cells.

141 **Oligonucleotides.** All padlock probes, primers and dual-labeled probes were  
142 synthesized by Integrated DNA Technologies, Inc. Padlock probes containing a 5'-  
143 phosphate group were chemically synthesized by standard phosphoramidite chemistry  
144 and purified by polyacrylamide gel electrophoresis by the manufacturer. All of the  
145 probes used in this study were 83-mers containing the following common spacer region  
146 of 49 bases

147 (5'-TTGCGACTCGTCATGTCTGAACTCTAGTGATCTTAGTGTCAGGATAGCT-  
148 3'). The target arms were directed against various minus- and plus-strand sites in pHDV-  
149 EGFP.

150 Amplification of ligated probes was performed using RCA-23 as the forward  
151 primer (5'-ACTAGAGTTCAGACATGACGAGT-3') and REV-21 as the reverse primer  
152 (5'-GATCTTAGTGTCAGGATAGCT-3'). These primers were chemically synthesized  
153 with a 5'-OH. Dual-labeled probes used for real-time quantitative PCR were end-labeled  
154 with 5'-FAM and 3'-TAMRA.

155 **SSA assay.** During the first step of SSA, a padlock probe was hybridized to a  
156 denatured target DNA and circularized by treatment with thermostable *Taq* DNA ligase  
157 (New England Biolabs). The 10- $\mu\text{l}$  reaction mix contained 1X *Taq* DNA ligase buffer,  
158  $10^9$  molecules of padlock probe, 12 units of *Taq* DNA ligase and 4  $\mu\text{l}$  of total cellular

159 DNA extracted from infected cells as described above. After an initial incubation at 95  
160 °C for 5 min to denature the target DNA, ligation was performed during 20 cycles of  
161 denaturing at 95 °C for 1 min and probe annealing and ligation at 50 °C for 4 min,  
162 followed by a final incubation at 50 °C for 10 min. Negative control reactions were  
163 prepared as above except that either target DNA or *Taq* DNA ligase was omitted. For  
164 each of the 12 padlock probes, the ligation reactions were performed using serial  
165 dilutions of linearized pHDV-EGFP DNA and 25 ng of uninfected 293T cell DNA to  
166 generate a standard curve in order to calculate the copy numbers of target DNA samples.

167 Detection of ligated padlock probe products was monitored by first subjecting  
168 dilutions of the ligation reaction to a modified RCA method using two primers, followed  
169 by quantitative real-time PCR using dual-labeled probes. Ligation reactions were diluted  
170 to 100 µl with water and 5-µl aliquots were added to a reaction mixture (25 µl, final  
171 volume) containing 20 mM Tris-HCl (pH 8.8), 10 mM KCl, 10 mM (NH<sub>4</sub>)<sub>2</sub>SO<sub>4</sub>, 2 mM  
172 MgSO<sub>4</sub>, 0.1% Triton X-100, 200 µM dNTPs, 500 nM each of RCA-23 (forward) and  
173 REV-21 (reverse) primers, 100 nM dual-labeled probe, 1 unit of Platinum *Taq* DNA  
174 polymerase (Invitrogen) and 2.4 units of *Bst* DNA polymerase (large fragment; New  
175 England Biolabs). An initial incubation was performed at 63 °C for 8 min for the two-  
176 primer RCA reaction, followed by two min incubation at 94 °C, which effectively  
177 denatured *Bst* DNA polymerase while simultaneously activating Platinum *Taq* DNA  
178 polymerase. Samples were then subjected to 40 cycles of PCR (94 °C for 15 sec and 60-  
179 63 °C for 1 min). Fluorescence data was collected during the extension step using an  
180 ABI PRISM 7700 Sequence Detection System. Copy numbers of target DNA were

181 calculated using the ABI PRISM 7700 Sequence Detection System software based on  
182 standard curves generated with serial dilutions of pHDV-EGFP in the ligation reactions.

183 To normalize for the amount of input DNA added to an SSA reaction, samples  
184 were measured by conventional real-time PCR, using a primer-probe set specific for the  
185 the cellular porphobilinogen deaminase (PBGD) gene (Genbank accession number  
186 M95623) (27) as previously described (25). The forward primer was 5'-  
187 AGGGATTCACTCAGGCTCTTTCT-3', the reverse primer was 5'-  
188 GCATGTTCAAGCTCCTTGGTAA-3' and the probe was 5'-FAM-  
189 TCCGGCAGATTGGAGAGAAAAGCCTG-TAMRA-3'. Final copy numbers after  
190 PBGD normalization and subtraction of 0-h copy numbers are expressed as the  
191 percentage of the 6-h copy number.

192 The kinetics of minus-strand DNA transfer and initiation of plus-strand DNA  
193 synthesis at the PPT were determined by using probes 1, 2 and 7, which detect reverse  
194 transcription products derived from the LTRs; during reverse transcription, the 3' LTR is  
195 first synthesized soon after minus-strand DNA transfer and the 5' LTR is synthesized  
196 after plus-strand DNA transfer. The kinetics of accumulation of LTR products over the  
197 6-h time course represents synthesis of both LTRs; analysis of the kinetics of  
198 accumulation of LTR-specific probes suggested that most of the synthesis of the 3' LTR  
199 is completed within the first 3 h after infection. Therefore, the kinetics of minus-strand  
200 DNA transfer and plus-strand DNA synthesis initiation at the PPT were analyzed over a  
201 time course of 3 h instead of 6 h. Finally, the copy numbers of the minus-strand DNA  
202 products detected by probe 4, which are complementary to the central flap on the plus-  
203 strand DNA, were similar to those detected with probe 1.

204

205

## RESULTS

206

207 **Strategy for SSA assay.** SSA is based on the use of single-stranded padlock probes,  
208 which specifically hybridize to a target strand at their 5' and 3' ends (14) (FIG. 1A).  
209 After infection with HIV-1, total cellular DNA (including nascent HIV-1 DNA) is  
210 isolated, denatured, and hybridized to a strand-specific padlock probe. The probe termini  
211 are ligated to form a circularized probe that is amplified using cascade rolling-circle  
212 amplification (RCA) (11, 21). The products of this reaction are quantified by real-time  
213 PCR using dual-labeled TaqMan probes (6). Twelve padlock probes (FIG. 1B and 1C)  
214 were designed to allow measurements of the kinetics of minus-strand DNA transfer  
215 (probes 1 and 2), minus-strand DNA synthesis (probes 3, 4, 5 and 6), plus-strand DNA  
216 synthesis initiation at the polypurine tract (PPT; probes 2 and 7) and central polypurine  
217 tract (cPPT; probes 5 and 11), plus-strand DNA transfer (probes 6 and 8), plus-strand  
218 DNA synthesis (probes 8, 9, 11 and 12), and detection and quantification of the central  
219 flap (probe 10).

220 **Determination of the sensitivity and accuracy of the SSA assay.** To analyze  
221 the kinetics of HIV-1 reverse transcription, we generated VSV-G-pseudotyped HDV-  
222 EGFP virions by transfection with pHCMV-G of HIV-GFP2, a 293T-based cell line  
223 containing proviral copies of HDV-EGFP. The accuracy of quantitative real-time PCR  
224 assays is often compromised by contamination with the plasmid DNA used during  
225 transfection. To avoid this source of contamination, we used producer cells in which the  
226 viral DNA was stably integrated in to the host cell chromosomal DNA. Another potential

227 source of DNA contamination was reinfection of the viral producer cells, leading to  
228 reverse transcription and formation of viral DNA products after transfection with VSV-  
229 G- expressing plasmid. To suppress this possible source of DNA contamination, we  
230 maintained the producer cells in the presence of AZT to suppress reinfection of the  
231 producer cells.

232 The efficiency and background of SSA assay were determined for each of the 12  
233 probes shown in Figs. 1B and 1C; representative results obtained from SSA analysis  
234 using probe 9 are shown in Table 1. High copy numbers of HIV-1-specific products ( $2 -$   
235  $6 \times 10^6$ ) were detected 6 h after infection per SSA reaction, while the background copy  
236 numbers for 0 h control were less than 0.1% (313 copies), providing a strong signal-to-  
237 noise ratio. For some probes the background signals were higher, but never exceeded 1%  
238 (data not shown).

239 To estimate reproducibility of SSA assay the kinetics of accumulation of reverse  
240 transcription products detected with specific probes was determined in four independent  
241 experiments. Representative results obtained for probe 9 are shown in Table 2. For most  
242 experiments, the standard deviations were less than 20% of the average.

243 To control for efficiency of total DNA recovery, the copy numbers of the PBGD  
244 gene (27) were determined, which were within threefold of each other in most  
245 experiments, and used to normalize the levels of reverse transcription products. Analysis  
246 of reverse transcription products 6, 12, and 24 h post-infection indicated that the amount  
247 of viral DNA products peaked at 6 h (data not shown). Therefore, the PBGD-normalized  
248 copy numbers at 6 h post-infection were set to 100% and the copy numbers obtained at  
249 earlier time points were expressed as a percentage of the 6 h copy numbers. In order to

250 plot the kinetics of accumulation of reverse transcription products on a log scale, values  
251 less than 1% of the copy numbers obtained 6 h post-infection were set to 1%.

252 For analysis and comparison of data obtained from independent PCR reactions,  
253 the standard curves were generated by using the padlock probes to detect serially diluted  
254 samples containing known copy numbers of the target DNA (black circles) and  
255 experimental samples (red circles); representative standard curves obtained for probes 3  
256 and 11 are shown in Fig. 2A. The correlation coefficients were  $>0.99$ , indicating that the  
257 output signals were linear with respect to input DNA. All 12 strand-specific padlock  
258 probes reproducibly generated similar standard curves, indicating linear output signals.  
259 Note that the efficiency of amplification for all probes was different as demonstrated for  
260 probe 3 and 11. For example, the observation that the signal for the known sample  
261 containing  $10^7$  copies was detected at cycle 14 by probe 3 and cycle 12 by probe 11  
262 indicated that binding to the target sequence, efficiency of ligation, and/or efficiency of  
263 amplification with probe 3 is less efficient than with probe 11. Nevertheless, because the  
264 copy numbers in target DNAs were estimated from the standard curves, the efficiency of  
265 amplification does not influence the quantitation of target DNA copies.

266 The viral DNA copy numbers obtained using SSA were compared to the copy  
267 numbers obtained using an early RT primer probe set (R-U5) and standard quantitative  
268 real-time PCR (Table 3). The results showed that the copy numbers obtained using SSA  
269 were similar to those obtained using quantitative real time PCR except for the 0 h time  
270 point, because the background copy numbers using SSA were generally between 100 –  
271 1000 copies; thus, the SSA method does not have the sensitivity to accurately detect copy  
272 numbers below 1000, but in samples containing higher copy numbers, the values

273 obtained with SSA are comparable to those obtained with standard quantitative real-time  
274 PCR.

275 **The rate of minus-strand DNA synthesis in 293T and primary human CD4<sup>+</sup>**

276 **T cells.** To determine the rate of minus-strand DNA synthesis, we performed SSA  
277 analysis with probes 3 and 6; representative experiments are shown in FIG. 2B using  
278 293T cells (left panel) and activated human primary CD4<sup>+</sup> T cells (right panel). The  
279 accumulation of reverse transcription products detected with each probe was expressed as  
280 a percentage of the copy number of products that accumulated at the 6-h time point. The  
281 distance between the curves representing the kinetics of accumulation of the products  
282 provided an estimate of the average time required for RT to copy the template between  
283 two probes. The average distance between the linear portions of the curves was  
284 determined by measuring the distance when the amounts of products accumulated were 5,  
285 10, 20, and 30% (shown as red arrows).

286 The representative experiments displayed in Fig 2B showed that time required for  
287 minus-strand DNA synthesis to be extended from probe 3 to probe 6 (7,031 nt) was  
288 approximately 105 min for 293T cells and 104 minutes for human primary CD4<sup>+</sup> T cells,  
289 providing overall rates of DNA synthesis of 67 and 68 nt/min, respectively. In 293T  
290 cells, the average rate of minus-strand DNA synthesis for five independent experiments,  
291 using probes 3 and 6 was  $68 \pm 17$  nt/min, requiring an average of  $109 \pm 30$  min (Table 4).  
292 In activated primary CD4<sup>+</sup> T cells, the average rate of minus-strand DNA synthesis for  
293 three independent experiments was  $70$  nt/min  $\pm 3$  min, requiring an average of  $101$  min  $\pm$   
294  $5$  min. Thus, the rates of minus-strand DNA synthesis were very similar in 293T cells  
295 and activated primary CD4<sup>+</sup> T cells.

296 **Kinetics of minus- and plus-strand DNA transfer.** The kinetics of product  
297 accumulation detected by probes 1 and 2 and probes 6 and 8 were compared after  
298 infection of 293T cells to estimate the average time required for minus- and plus-strand  
299 DNA transfer, respectively. On average, ~11 min were required for extension of minus-  
300 strand DNA synthesis from probe 1 in U5 to probe 2 in U3 (FIG. 2C, left panel). At a  
301 rate of DNA synthesis of ~68 nt/min, approximately ~7 min were required for copying  
302 the 490 nt between probes 1 and 2. Since extension of minus-strand DNA synthesis from  
303 probe 1 to probe 2 required ~11 min, a delay of ~4 min (~11 min - ~7 min) was  
304 associated with minus-strand DNA transfer.

305 Similarly, we determined the kinetics of plus-strand DNA transfer after infection  
306 of 293T cells by analyzing the accumulation of products detected by probes 6 and 8,  
307 which are located 3' of the PBS and are specific for the minus and plus strand,  
308 respectively (FIG. 2C, right panel). On average, ~28 min were required for reverse  
309 transcription to proceed from probe 6 to probe 8. Since ~100 nt of DNA synthesis  
310 occurred during progression of reverse transcription from probe 6 to probe 8, requiring  
311 approximately 2 min for synthesis, a longer delay of ~26 min (~28 min - ~2 min) was  
312 associated with plus-strand DNA transfer.

313 **Kinetics of plus-strand DNA synthesis initiation.** The kinetics of initiation of  
314 plus-strand DNA synthesis at the PPT after infection of 293T cells were determined by  
315 analyzing the accumulation of products detected by probes 2 and 7, which are located 3'  
316 of the PPT and are specific for the minus- and plus-strand, respectively (FIG. 2D, left  
317 panel). On average, ~12 min were needed for progression of reverse transcription from  
318 probe 2 to probe 7. Approximately 3 min (~68 nt/min) were required to incorporate ~200

319 nt during progression of reverse transcription from probe 2 to probe 7. Thus, a delay of  
320 ~9 min (~12 min – ~3 min) was associated with initiation of plus-strand DNA synthesis  
321 at the PPT.

322 Similarly, the kinetics of plus-strand DNA synthesis initiation at the cPPT was  
323 determined by analyzing the accumulation of products detected by probes 5 and 11 (FIG.  
324 2D, right panel). An average of ~31 min was required for progression of reverse  
325 transcription from probe 5 to probe 11 whereas DNA synthesis (~200 nt) required ~3 min  
326 (~68 nt/min). Thus, a longer delay of ~28 min was associated with initiation of plus-  
327 strand DNA synthesis at the cPPT in comparison to the PPT.

ACCEPTED

328 **Plus-strand DNA synthesis is initiated at multiple sites.** To determine the rate  
329 of plus-strand DNA synthesis in 293T cells, we compared the kinetics of accumulation of  
330 products detected by plus-strand-specific probes 8, 9, 11 and 12 (FIG. 3A). The products  
331 detected by probes 11 and 12 accumulated with faster kinetics than products detected by  
332 probes 8 and 9, indicating that plus-strand DNA synthesis initiation at the cPPT and  
333 subsequent plus-strand DNA synthesis through probe 11 and 12 sites occurred ~30 min  
334 before minus-strand DNA synthesis reached the PBS to allow plus-strand DNA transfer  
335 and synthesis of products detected by probes 8 and 9. Probes 8 and 9 are 5' of the cPPT  
336 and are separated by 4,060 nt whereas probes 11 and 12 are 3' of the central termination  
337 signal (CTS) and are separated by 2,759 nt. Despite the long distances separating these  
338 probes, the products detected by probes 8 and 9 accumulated with very similar kinetics,  
339 as did those of probes 11 and 12, implying either a very fast rate of plus-strand DNA  
340 synthesis or the presence of multiple sites for DNA synthesis initiation.

341 To determine whether additional sites of plus-strand DNA synthesis initiation  
342 contribute to the accumulation of plus-strand DNA products, we generated a cPPT<sup>-</sup>  
343 mutant by introducing four purine-to-pyrimidine substitutions within the cPPT sequence.  
344 The mutations in the cPPT did not significantly influence its ability to complete a single  
345 cycle of replication as determined by analysis of GFP expression in infected cells (data  
346 not shown). We observed that after infection with the cPPT<sup>-</sup> mutant, the products  
347 detected with probe 12 accumulated with faster kinetics than the products detected with  
348 probe 11 (FIG. 3B), indicating that plus-strand DNA synthesis was initiated at one or  
349 more sites between probes 11 and 12. Plus-strand DNA synthesis initiation at the cPPT  
350 was abrogated by the mutations in the cPPT, because probe 11 products accumulated

351 with kinetics similar to those for probe 8 and 9 rather than with the faster kinetics  
352 observed when the cPPT was wild type (FIG. 3A).

353 A comparison of the copy numbers of viral DNA products accumulated 6 h post-  
354 infection indicated similar copy numbers for most of the products (within twofold),  
355 indicating that after minus-strand DNA synthesis was initiated, the process of reverse  
356 transcription was efficient (FIG. 3C, blue bars).

357 In contrast to most of the reverse transcription products, the product detected with  
358 probe 10 accumulated to a two- to threefold higher copy number level than the product  
359 detected by probe 1. Probe 10 was designed to detect the central flap (FIG. 1B), and two  
360 copies of probe 10 product were expected to be generated during reverse transcription;  
361 one copy would result from initiation at the cPPT and a second copy would result from  
362 plus-strand strong-stop DNA transfer followed by extension of plus-strand DNA  
363 synthesis, leading to displacement of the synthesized DNA initiating at the cPPT. The  
364 detection of two to three copies of the products detected with probe 10 in comparison to  
365 the plus-strand DNA products detected with probes 9 and 11, which flank the central flap,  
366 indicated that the SSA analysis was able to quantitatively distinguish between one and  
367 two copies of reverse transcription products. As predicted, mutation of the cPPT (FIG.  
368 3C, red bars) resulted in a lower copy number of products detected by probe 10 in  
369 comparison to the wild type, indicating that the central flap was no longer formed.

370 **Effects of RT inhibitors on minus- and plus-strand DNA synthesis.** To  
371 determine whether inhibitors of HIV-1 RT display differential effects during minus- and  
372 plus-strand DNA synthesis, we performed time-course experiments in the presence of the  
373 nucleoside RT inhibitors (NRTIs) 2',3'-dideoxyinosine (ddI), 3'-deoxy-2',3'-

374 didehydrothymidine (d4T) and 3'-azido-3'-deoxythymidine (AZT) and the nonnucleoside  
375 RT inhibitor (NNRTI) efavirenz (EFV) at concentrations that inhibited viral replication  
376 by 97-99% (Table 5 and FIG. 4). The inhibition of viral replication was monitored by  
377 performing FACS analysis to determine the percentage of infected cells that expressed  
378 GFP. The RT inhibitors had a minimal effect on the early minus-strand DNA products  
379 detected by probe 3 (FIG. 4A, right panel); in contrast, the late minus-strand DNA  
380 products detected by probe 6 accumulated to variable levels (FIG. 4A, left panel). In the  
381 presence of AZT and d4T, the probe 6 products accumulated to approximately 5% of the  
382 control levels; in comparison, the probe 6 products accumulated to approximately 15 and  
383 55% of the control in the presence of EFV and ddI, respectively. Thus, minus-strand  
384 DNA synthesis was substantially inhibited by AZT and d4T, moderately inhibited by  
385 EFV and minimally inhibited by ddI.

386 The accumulation of plus-strand DNA products detected by probes 8 and 9 (FIG.  
387 4B, left panels) was inhibited to a similar extent as compared to the probe 6 products  
388 (FIG. 4A, left panel), whereas the accumulation of products detected with probes 11 and  
389 12 (FIG. 4B, right panels) was inhibited to a similar extent as compared to the probe 3  
390 products (FIG. 4A, right panel). This suggested a parallel between the accumulation of  
391 plus-strand DNA products and complementary minus-strand DNA products, which was  
392 most clearly evident for probes 6 and 8; for example, AZT and d4T inhibited the  
393 accumulation of probe 6 products to 5% of the control and a similar level of inhibition of  
394 probe 8 products was observed. Similarly, the accumulation of products detected by  
395 probes 11 and 12 was only modestly inhibited in the presence of RT inhibitors and was  
396 similar to the accumulation of probe 3 products (FIG. 4A); because a greater percentage

397 of minus-strand DNA products were likely extended past the probe 11 and 12 binding  
398 sites, initiation at the cPPT or other internal sites may have resulted in higher levels of  
399 accumulation of probe 11 and 12 products than probe 8 and 9 products.

400 These results showed that AZT and d4T inhibited minus-strand DNA synthesis by  
401 95% at drug concentrations that inhibited viral replication by 98% (approximately 20-  
402 fold). The observation that most of the inhibition of viral replication could be accounted  
403 for by the inhibition of minus-strand DNA synthesis suggests the intriguing possibility  
404 that AZT and d4T inhibited reverse transcription primarily during minus-strand DNA  
405 synthesis. However, inhibition of plus-strand DNA synthesis by AZT and d4T cannot be  
406 excluded. ddI and EFV inhibited minus-strand DNA synthesis by 45% and 85%,  
407 respectively, at drug concentrations that inhibited viral replication by >95%, implying  
408 that these RT inhibitors also impaired plus-strand DNA synthesis. Inhibition of plus-  
409 strand DNA synthesis could not be observed in these studies because it is initiated at  
410 multiple sites and reduction in plus-strand products is not cumulative, as is the case for  
411 minus-strand DNA synthesis.

412

## 413 **DISCUSSION**

414

415 The novel SSA assay described here should be applicable to a wide range of  
416 molecular studies in which quantification of specific strands of nucleic acids is desirable,  
417 including replication of other viruses (hepadnaviruses, adenoviruses, herpesviruses, etc.)  
418 and leading- and lagging-strand synthesis in organisms with double-stranded genomes.  
419 The SSA assay now further advances the quantitative PCR technology that has been

420 applied to the measurements of HIV-1 viral load (3, 17), integrated DNA copies (2), and  
421 reverse transcription kinetics (2, 8, 24) by providing a tool for analyzing the strand-  
422 specific aspects of viral replication.

423 To our knowledge, these studies have provided the first measurements of several  
424 key steps during HIV-1 replication in cells, including the rate of minus-strand DNA  
425 synthesis (~68-70 nt/min). Previous measurements based on *in vitro* assays using either  
426 purified HIV-1 RTs (5, 7, 9, 12, 18) or endogenous reactions using components from  
427 permeabilized virions (1, 19, 23) varied greatly from 30-5000 nt/min, presumably  
428 because the rates of DNA synthesis can be influenced by the assay conditions. The  
429 kinetics of HIV-1 replication probably also depend on intracellular conditions (15) and  
430 may exhibit cell-specific differences. Interestingly, the rates we obtained here for 293T  
431 cells and activated human primary CD4<sup>+</sup> T cells were very similar, suggesting that  
432 intracellular conditions such as dNTP concentration are similar in these two cell types.  
433 However, we noted a delay in the kinetics for both probes 3 and 6 in human primary  
434 CD4<sup>+</sup> T cells, suggesting a possible delay in viral entry and early post-entry steps such as  
435 uncoating, delay in initiation of minus-strand DNA synthesis, or a delay in minus-strand  
436 DNA transfer (FIG. 2A). The SSA assay can also be used to determine the effects of  
437 specific mutations in viral proteins (RT, NC, Vif, Vpr, Nef, etc.) as well as *cis*-acting  
438 elements (PBS, PPT, cPPT, CTS, etc.) on the kinetics of various steps in HIV-1  
439 replication.

440 The mechanism(s) that might contribute to the regional differences in the rate of  
441 minus-strand DNA synthesis are not known but could involve template RNA structures  
442 or greater availability of nucleocapsid (NC) protein later in replication, leading to more

443 efficient denaturation of template structures, thereby increasing the rate of reverse  
444 transcription. The observation that plus-strand DNA transfer (~26 min) is much slower  
445 than minus-strand DNA transfer (~4 min) suggests that tRNA primer removal might be a  
446 slow and rate limiting step. The observation that plus-strand initiation at the cPPT (~28  
447 min) was much slower than at the PPT (~8 min) suggests that differences in sequences  
448 surrounding the two identical PPTs can influence the kinetics with which these plus-  
449 strand initiation sites are utilized.

450 Analysis of the cPPT<sup>-</sup> mutant of HIV-1 and the similar kinetics with which plus-  
451 strand products separated by long distances accumulated has provided strong evidence  
452 for multiple sites of plus-strand DNA synthesis initiation during replication in cells, as  
453 previously reported (10, 13). It is unclear at this time how many additional sites are used  
454 to initiate plus-strand DNA synthesis during HIV-1 replication, whether they represent  
455 specific sequences or RNA fragments that remain randomly associated with the minus-  
456 strand DNA, and how they avoid being displaced by DNA synthesis initiated at upstream  
457 sites.

458 Our observation that probe 10 products specifically detected two- to threefold  
459 higher copy numbers of the central flap sequence, which has been implicated in the  
460 nuclear transport of HIV-1 preintegration complexes (20, 28), indicates that the SSA  
461 assay can provide a quantitative method for the detection of the central flap and could be  
462 used to analyze the efficiency of displacement synthesis in other regions of the HIV-1  
463 genome.

464 In these studies, the inhibition of viral replication by AZT, d4T, and ddI was  
465 similar (97-99%), representing inhibition of minus- and plus-strand DNA synthesis. For

466 AZT and d4T, most of the inhibition of viral replication could be attributed to the  
467 observed 95% inhibition of minus-strand DNA synthesis. However, ddI treatment  
468 resulted in 55% inhibition of minus-strand DNA synthesis, suggesting that ddI also  
469 inhibited viral replication during plus-strand DNA synthesis.

470 In summary, the SSA method should provide a widely applicable technology for  
471 strand-specific analysis of nucleic acids. The SSA assay described here can be used to  
472 address a variety of questions about the process of HIV-1 replication, elucidate the  
473 mechanism of action of antiretroviral agents, and facilitate development of novel antiviral  
474 agents that interfere with specific steps in HIV-1 reverse transcription.

#### 475 476 **ACKNOWLEDGMENTS**

477 We thank Anne Arthur for expert editorial help. We also thank Rebekah Barr and  
478 Hongzhan Xu for technical assistance and Krista Delviks-Frankenberry and Eric Freed  
479 for critical reading of the manuscript. This research was supported in part by the  
480 Intramural Research Program of the NIH, National Cancer Institute, Center for Cancer  
481 Research. This project has been funded in whole or in part with federal funds from the  
482 National Cancer Institute, National Institutes of Health, under contract N01-CO-12400.  
483 The content of this publication does not necessarily reflect the views or policies of the  
484 Department of Health and Human Services, nor does mention of trade names,  
485 commercial products, or organizations imply endorsement by the U.S. Government.

486

## REFERENCES

487

488

- 489 1. **Boone, L. R., and A. M. Skalka.** 1981. Viral DNA synthesized in vitro by avian  
490 retrovirus particles permeabilized with melittin. I. Kinetics of synthesis and size  
491 of minus- and plus-strand transcripts. *J Virol* **37**:109-16.
- 492 2. **Butler, S. L., M. S. Hansen, and F. D. Bushman.** 2001. A quantitative assay for  
493 HIV DNA integration in vivo. *Nat Med* **7**:631-4.
- 494 3. **Cesaire, R., A. Dehee, A. Lezin, N. Desire, O. Bourdonne, F. Dantin, O. Bera,**  
495 **D. Smadja, S. Abel, A. Cabie, G. Sobesky, and J. C. Nicolas.** 2001.  
496 Quantification of HTLV type I and HIV type I DNA load in coinfecting patients:  
497 HIV type 1 infection does not alter HTLV type I proviral amount in the peripheral  
498 blood compartment. *AIDS Res Hum Retroviruses* **17**:799-805.
- 499 4. **Coffin, J. M., Hughes, S.H & Varmus, H.E.** 1997. *Retroviruses.* Cold Spring  
500 Harbor Laboratory Press, Cold Spring Harbor, New York.
- 501 5. **Dube, D. K., and L. A. Loeb.** 1976. On the association of reverse transcriptase  
502 with polynucleotide templates during catalysis. *Biochemistry* **15**:3605-11.
- 503 6. **Holland, P. M., R. D. Abramson, R. Watson, and D. H. Gelfand.** 1991.  
504 Detection of specific polymerase chain reaction product by utilizing the 5'----3'  
505 exonuclease activity of *Thermus aquaticus* DNA polymerase. *Proc Natl Acad Sci*  
506 *U S A* **88**:7276-80.
- 507 7. **Huber, H. E., J. M. McCoy, J. S. Seehra, and C. C. Richardson.** 1989. Human  
508 immunodeficiency virus 1 reverse transcriptase. Template binding, processivity,  
509 strand displacement synthesis, and template switching. *J Biol Chem* **264**:4669-78.

- 510 8. **Karageorgos, L., P. Li, and C. J. Burrell.** 1995. Stepwise analysis of reverse  
511 transcription in a cell-to-cell human immunodeficiency virus infection model:  
512 kinetics and implications. *J Gen Virol* **76 ( Pt 7)**:1675-86.
- 513 9. **Kati, W. M., K. A. Johnson, L. F. Jerva, and K. S. Anderson.** 1992.  
514 Mechanism and fidelity of HIV reverse transcriptase. *J Biol Chem* **267**:25988-97.
- 515 10. **Klarmann, G. J., H. Yu, X. Chen, J. P. Dougherty, and B. D. Preston.** 1997.  
516 Discontinuous plus-strand DNA synthesis in human immunodeficiency virus type  
517 1-infected cells and in a partially reconstituted cell-free system. *J Virol* **71**:9259-  
518 69.
- 519 11. **Lizardi, P. M., X. Huang, Z. Zhu, P. Bray-Ward, D. C. Thomas, and D. C.**  
520 **Ward.** 1998. Mutation detection and single-molecule counting using isothermal  
521 rolling-circle amplification. *Nat Genet* **19**:225-32.
- 522 12. **Majumdar, C., J. Abbotts, S. Broder, and S. H. Wilson.** 1988. Studies on the  
523 mechanism of human immunodeficiency virus reverse transcriptase. Steady-state  
524 kinetics, processivity, and polynucleotide inhibition. *J Biol Chem* **263**:15657-65.
- 525 13. **Miller, M. D., B. Wang, and F. D. Bushman.** 1995. Human immunodeficiency  
526 virus type 1 preintegration complexes containing discontinuous plus strands are  
527 competent to integrate in vitro. *J Virol* **69**:3938-44.
- 528 14. **Nilsson, M., H. Malmgren, M. Samiotaki, M. Kwiatkowski, B. P.**  
529 **Chowdhary, and U. Landegren.** 1994. Padlock probes: circularizing  
530 oligonucleotides for localized DNA detection. *Science* **265**:2085-8.
- 531 15. **O'Brien, W. A., A. Namazi, H. Kalhor, S. H. Mao, J. A. Zack, and I. S. Chen.**  
532 1994. Kinetics of human immunodeficiency virus type 1 reverse transcription in

- 533 blood mononuclear phagocytes are slowed by limitations of nucleotide precursors.  
534 J Virol **68**:1258-63.
- 535 16. **O'Doherty, U., W. J. Swiggard, and M. H. Malim.** 2000. Human  
536 immunodeficiency virus type 1 spinoculation enhances infection through virus  
537 binding. J Virol **74**:10074-80.
- 538 17. **Palmer, S., A. P. Wiegand, F. Maldarelli, H. Bazmi, J. M. Mican, M. Polis, R.**  
539 **L. Dewar, A. Planta, S. Liu, J. A. Metcalf, J. W. Mellors, and J. M. Coffin.**  
540 2003. New real-time reverse transcriptase-initiated PCR assay with single-copy  
541 sensitivity for human immunodeficiency virus type 1 RNA in plasma. J Clin  
542 Microbiol **41**:4531-6.
- 543 18. **Reardon, J. E.** 1993. Human immunodeficiency virus reverse transcriptase. A  
544 kinetic analysis of RNA-dependent and DNA-dependent DNA polymerization. J  
545 Biol Chem **268**:8743-51.
- 546 19. **Rothenberg, E., and D. Baltimore.** 1977. Increased length of DNA made by  
547 virions of murine leukemia virus at limiting magnesium ion concentration. J Virol  
548 **21**:168-78.
- 549 20. **Sirven, A., F. Pflumio, V. Zennou, M. Titeux, W. Vainchenker, L.**  
550 **Coulombel, A. Dubart-Kupperschmitt, and P. Charneau.** 2000. The human  
551 immunodeficiency virus type-1 central DNA flap is a crucial determinant for  
552 lentiviral vector nuclear import and gene transduction of human hematopoietic  
553 stem cells. Blood **96**:4103-10.

- 554 21. **Thomas, D. C., G. A. Nardone, and S. K. Randall.** 1999. Amplification of  
555 padlock probes for DNA diagnostics by cascade rolling circle amplification or the  
556 polymerase chain reaction. *Arch Pathol Lab Med* **123**:1170-6.
- 557 22. **Unutmaz, D., V. N. KewalRamani, S. Marmon, and D. R. Littman.** 1999.  
558 Cytokine signals are sufficient for HIV-1 infection of resting human T  
559 lymphocytes. *J Exp Med* **189**:1735-46.
- 560 23. **Varmus, H. E., S. Heasley, H. J. Kung, H. Oppermann, V. C. Smith, J. M.**  
561 **Bishop, and P. R. Shank.** 1978. Kinetics of synthesis, structure and purification  
562 of avian sarcoma virus-specific DNA made in the cytoplasm of acutely infected  
563 cells. *J Mol Biol* **120**:55-82.
- 564 24. **Victoria, J. G., D. J. Lee, B. R. McDougall, and W. E. Robinson, Jr.** 2003.  
565 Replication kinetics for divergent type 1 human immunodeficiency viruses using  
566 quantitative SYBR green I real-time polymerase chain reaction. *AIDS Res Hum*  
567 *Retroviruses* **19**:865-74.
- 568 25. **Voronin, Y. A., and V. K. Pathak.** 2004. Frequent dual initiation in human  
569 immunodeficiency virus-based vectors containing two primer-binding sites: a  
570 quantitative in vivo assay for function of initiation complexes. *J Virol* **78**:5402-  
571 13.
- 572 26. **Yee, J. K., A. Miyanojara, P. LaPorte, K. Bouic, J. C. Burns, and T.**  
573 **Friedmann.** 1994. A general method for the generation of high-titer, pantropic  
574 retroviral vectors: highly efficient infection of primary hepatocytes. *Proc Natl*  
575 *Acad Sci U S A* **91**:9564-8.

- 576 27. **Yoo, H. W., C. A. Warner, C. H. Chen, and R. J. Desnick.** 1993.  
577 Hydroxymethylbilane synthase: complete genomic sequence and amplifiable  
578 polymorphisms in the human gene. *Genomics* **15**:21-9.
- 579 28. **Zennou, V., C. Petit, D. Guetard, U. Nerhbass, L. Montagnier, and P.**  
580 **Charneau.** 2000. HIV-1 genome nuclear import is mediated by a central DNA  
581 flap. *Cell* **101**:173-85.
- 582
- 583

ACCEPTED

**FIGURE LEGENDS**

584

585

586 FIG. 1. SSA method for analysis of minus- and plus-strand DNA synthesis during HIV-1  
587 reverse transcription. (A) Experimental strategy for SSA analysis. First (upper left), a  
588 single-stranded oligonucleotide (padlock probe) is hybridized at the 5' and 3' ends to one  
589 strand of a target nucleic acid (blue arrow). In this example, the padlock probe is shown  
590 as hybridizing to the minus-strand DNA adjacent to the PPT. Second, the 5' and 3' ends  
591 of the padlock probe are ligated to form a covalently closed circular DNA (blue square).  
592 A primer (black bar) is annealed to the circularized probe. Third, the circularized probe  
593 is amplified using a rolling-circle amplification protocol. A second primer (open bar)  
594 that anneals to the long single-stranded molecule generated through rolling-circle  
595 amplification is added to the reaction to exponentially amplify the probe sequences in a  
596 cascade reaction. Finally, the ligation junctions present in the rolling- circle  
597 amplification reaction are quantified using a real-time PCR amplification protocol  
598 (primers are shown as black arrows and dual-labeled probes are labeled with green and  
599 red circles). (B) Padlock probes developed for SSA analysis of HIV-1 reverse  
600 transcription. A schematic outline of HIV-1 reverse transcription is presented. Solid  
601 black lines represent RNA, dashed black lines represent RNA degraded by the RNase H  
602 activity of RT and blue and red lines represent minus- and plus-strand DNAs,  
603 respectively. Abbreviations: R, repeat region; U5, unique 5' region; PBS, primer-binding  
604 site; cPPT, central polypurine tract; PPT, polypurine tract; U3, unique 3' region; CTS,  
605 central termination sequence. For simplicity, only one of the two copackaged viral  
606 genomic RNAs is shown. The approximate locations of the ligation sites for padlock

607 probes are indicated with numbers from 1 to 12 in color-coded boxes that are used  
608 throughout the figures. Probes 1 through 6 specifically detect minus-strand DNA  
609 products, whereas probes 7 through 12 specifically detect plus-strand DNA products. (C)  
610 As an example, partial sequence of padlock probe 1, the ligation junction (slash), and  
611 sequence of dual-labeled probe (underlined) are shown. The locations of the FAM (green  
612 F) and TAMRA (red T) fluorescent labels are indicated. A 49-base region that connects  
613 the target arms (spacer) is common to all probes. Probe 1 binds to a region that is located  
614 56 nt 5' of PBS.

615

616 Fig. 2. Determination of the kinetics of minus-strand DNA synthesis, minus- and plus-  
617 strand DNA transfer and initiation of plus-strand DNA synthesis using SSA analysis.

618 (A) Standard curves for padlock probes 3 and 11 used in SSA analysis. Serial dilutions  
619 of pHDV-EGFP ranging from  $4 \times 10^3$  –  $1 \times 10^7$  in the presence of 25 ng of uninfected  
620 293T cell DNA were subjected to SSA analysis to establish standard curves for padlock  
621 probes 3 (left panel) and 11 (right panel). Copy numbers of target DNA (red circles)  
622 were calculated using the ABI PRISM 7700 Sequence Detection System software based  
623 on the standard curve (black circles). (B) Rate of minus-strand DNA synthesis in 293T  
624 and human primary CD4<sup>+</sup> T cells. SSA analysis of HIV-1 reverse transcription using  
625 minus-strand specific padlock probes 3 and 6 is shown for time-course experiments  
626 performed with 293T cells (left panel) and human primary CD4<sup>+</sup> T cells (right panel).  
627 HDV-EGFP virus was used to infect 293T or human primary CD4<sup>+</sup> T cells and total  
628 cellular DNA was isolated from the infected cells at 30- or 60-min intervals for 6 h after  
629 infection. The accumulation of minus-strand DNA products detected with probes 3 and 6

630 was determined at each time point (see map above graph). The copy numbers of the  
631 products at 6 h after infection are set to 100% and the products at earlier time points are  
632 presented as a percentage of the copy numbers at the 6-h time point. To determine the  
633 rate at which reverse transcription proceeded from one probe to the next, the average  
634 distance between the curves (red arrows) generated for probes 3 and 6 was determined  
635 when the amounts of products accumulated were 5, 10, 20 and 30% of the 6-h time point.  
636 The time required for reverse transcription to proceed from probe 3 to probe 6 was  
637 approximately 105 and 104 min for 293T and human primary CD4<sup>+</sup> T cell time courses,  
638 respectively; since the distance between probes 3 and 6 is 7031 nt, the rate of DNA  
639 synthesis was 67 and 68 nt/min for the 293T and human primary CD4<sup>+</sup> T cell time  
640 courses, respectively. (C) Determination of the rates of minus- and plus-strand DNA  
641 transfer using SSA analysis in 293T cells. The kinetics of minus-strand DNA transfer  
642 (left graph) was determined by the same technique used for minus-strand DNA synthesis  
643 except that the accumulation of products detected by probes 1 and 2 (see map above the  
644 left graph) were determined over a 3-h time course. The average time required for  
645 reverse transcription to proceed from probe 1 to probe 2 (~11 min) was determined as  
646 described above. The distance between probes 1 and 2 is 490 nt (see map above the left  
647 graph). The kinetics of plus-strand DNA transfer (right graph) was determined by  
648 measuring the accumulation of products detected with probes 6 and 8 (~28 min) over a 6-  
649 h time course. (D) Determination of the kinetics of plus-strand initiation at the PPT and  
650 cPPT in 293T cells. Initiation of plus-strand DNA synthesis at the PPT (left graph) was  
651 determined by the same technique used for minus-strand DNA synthesis except that the  
652 accumulation of products detected with probes 2 and 7 (see map above graph) were

653 compared over a 3-h time course. Similarly, the kinetics of initiation of plus-strand DNA  
654 synthesis at the cPPT (right graph) was determined by analyzing the accumulation of  
655 products detected by probes 5 and 11 (see map above graph) over a 6-h time course. The  
656 average times indicated on each graph represent the delay in initiation of plus-strand  
657 DNA synthesis after minus-strand DNA synthesis has extended past the PPT (~12 min)  
658 and cPPT (~31 min).

659

660 FIG. 3. SSA analysis of plus-strand DNA synthesis. (A) The kinetics of plus-strand  
661 DNA synthesis after infection with wild-type HDV-EGFP were determined by comparing  
662 the accumulation of products detected with probes 8, 9, 11 and 12 (see map above graph).  
663 Products detected with probes 11 and 12 accumulated with faster kinetics than products  
664 detected with probes 8 and 9. (B) The kinetics of plus-strand DNA synthesis after  
665 infection with the cPPT<sup>-</sup> mutant of HDV-EGFP were determined by comparing  
666 accumulation of products detected with probes 8, 9, 11 and 12 (see map above graph in  
667 A). Products detected with probe 12 accumulated with faster kinetics than those detected  
668 with probes 8, 9 and 11. (C) Efficiency of reverse transcription of wild-type HDV-EGFP  
669 (blue bars) or the cPPT<sup>-</sup> mutant of HDV-EGFP (red bars). The copy numbers of reverse  
670 transcription products detected with probe 1 at 6 h were set to a value of 1 (average  
671 value:  $2-6 \times 10^6$  copies) and the copy numbers of products detected with various minus-  
672 and plus-strand probes (see FIG. 1B for location) are expressed relative to that of probe 1.  
673

674 Fig. 4. SSA analysis of the effect of RT inhibitors on minus- and plus-strand DNA  
675 synthesis. (A) Effects of RT inhibitors on minus-strand DNA synthesis. The

676 accumulation of products detected with probes 3 (right graph; see map above graph) and  
677 6 (left graph) are compared over a 6-h time period in the absence of drugs (No drug) or  
678 presence of ddi, EFV, d4T or AZT at concentrations that reduce viral titers by 95-99%  
679 (see Materials and Methods). (B) Effects of RT inhibitors on plus-strand DNA synthesis.  
680 The accumulation of products detected with probes 8 and 9 (left graphs) and 11 and 12  
681 (right graphs; see map above graph) are compared over a 6-h time period in the absence  
682 (No drug) or presence of RT inhibitors. The results in A and B are expressed as a  
683 percentage of the products accumulated at the 6-h time point in the absence of drugs.  
684 Legends are shown only for probes 3 but are the same for all probes.

ACCEPTED

685 Table 1. Time course for synthesis of HIV-1 plus-strand products detected by probe 9<sup>a</sup>

Time (hours)	HIV-1 DNA copy numbers <sup>b</sup>	PBGD copy numbers <sup>c</sup>	PBGD Normalization Factor <sup>d</sup>	PBGD-adjusted HIV-1 copy numbers <sup>d</sup>	PBGD-adjusted copy numbers – 0-h copy numbers <sup>e</sup>	% of 6-h HIV-1 copy number <sup>f</sup>
0	313	313,385	1	313	0	0.00
0.5	1,145	211,683	0.6755	1,695	1,382	0.07
1	1,648	297,392	0.949	1,737	1,424	0.07
1.5	4,827	236,076	0.7533	6,408	6,095	0.30
2	38,443	304,567	0.9719	39,554	39,243	1.90
2.5	137,888	309,238	0.9868	139,732	139,424	6.75
3	331,356	204,398	0.6522	508,059	507,726	24.58
3.5	471,427	187,171	0.5973	789,263	789,007	38.19
4	1,017,892	262,514	0.8377	1,215,103	1,214,828	58.80
5	1,602,039	261,303	0.8338	1,921,371	1,921,039	92.99
6	2,199,462	333,590	1.0645	2,066,193	2,065,930	100.00

686

687 <sup>a</sup>Table represents one of four sets of measurements performed for probe 9 samples.

688 <sup>b</sup>Copy numbers were calculated as described in Materials and Methods based on standard  
689 curves generated with known amounts of pHDV-EGFP in the presence of 25 ng of  
690 uninfected 293T cell DNA.

691 <sup>c</sup>PBGD copy numbers were determined as described in Materials and Methods.

692 <sup>d</sup> The PBGD normalization factors (column 4) were calculated by dividing the PBGD  
693 copy number at each time point with the PBGD copy number at the 0-h time point.

694 <sup>d</sup> PBGD-adjusted HIV-1 copy numbers (column 5) were determined by dividing the first  
695 the PBGD copy numbers (column 2) with the PBGD normalization factor (column 4).

696 <sup>e</sup>Final HIV-1 copy numbers (column 6) were calculated by subtracting the 0-h value  
697 (313) from the PBGD-adjusted copy numbers (column 5).

698 <sup>f</sup>Values were calculated as the percentage of the final copy numbers divided by the 6-h  
699 copy number (2,065,930) and placed in column 2 of Table 2.

700 Table 2. Summary of probe 9 copy numbers expressed as percentage of copy number at  
 701 six hours post-infection.

Time (Hours)	% of 6-h copy number- experiment 1 <sup>a</sup>	% of 6-h copy number- experiment 2	% of 6-h copy number- experiment 3	% of 6-h copy number- experiment 4	Avg. % of 6-h copy number (+/- STD) <sup>b</sup>
0	0.00	0.00	0.00	0.00	1
0.5	0.07	0.02	0.24	-0.05	1
1	0.07	0.12	0.04	-0.03	1
1.5	0.30	0.17	0.27	0.04	1
2	1.90	2.55	2.78	2.44	2.42 ± 0.37
2.5	6.75	7.59	9.94	10.31	8.64 ± 1.76
3	24.58	19.73	12.60	19.94	19.19 ± 4.92
3.5	38.19	41.35	31.49	27.75	34.66 ± 6.17
4	58.80	68.97	53.01	71.16	62.93 ± 8.59
5	92.99	110.08	96.72	90.86	97.66 ± 8.63
6	100.00	100	100	100	100

702

703 <sup>a</sup>Values were taken from last column of Table 1.

704 <sup>b</sup>Values represent average of four experiments (columns 2-5) and are expressed with  
 705 standard deviations. Values less than 1 are set to 1 in order to generate a log-scale graph.

706 Table 3. Comparison of real-time PCR and SSA analysis of time course for synthesis of  
 707 early HIV-1 products<sup>a</sup>

Time (hours)	PCR		SSA	
	Copy numbers <sup>b</sup>	% of 6-h copy <sup>c</sup> number	Copy numbers	% of 6-h copy number
0	465	0.03	1 <sup>d</sup>	1
1	73,386	5.86	123,816	6.57
2	463,205	36.96	867,267	46.02
3	645,744	51.52	1,596,262	84.69
4	842,297	67.20	1,434,647	76.12
5	1,422,299	113.48	1,955,951	103.78
6	1,253,384	100	1,884,744	100

708

709

710 <sup>a</sup>Early HIV-1 products were measured with an R-U5 primer-probe set for real-time PCR  
 711 analysis and padlock probe 1 (detecting minus-strand products) for SSA analysis. <sup>b</sup>Copy  
 712 numbers are averages of 2-4 sets of measurements performed using a standard curve and  
 713 normalized to PBGD copy numbers as described in the footnotes to Supplementary Table  
 714 1. <sup>c</sup> The % of 6-h copy number was calculated as the average copy number for each time  
 715 point divided by the 6-h copy number. <sup>d</sup>Note that the copy numbers for the 0-h time point  
 716 are not comparable because the SSA method does not have the sensitivity to detect copy  
 717 numbers below 1,000.

718 Table 4. Kinetics of HIV-1 minus-strand DNA synthesis<sup>a</sup>.

Time <sup>b</sup> Course	293T cells		Primary CD4 <sup>+</sup> T cells	
	Minutes	Rate <sup>c</sup> (nt/min)	Minutes	Rate (nt/min)
1	105	67	104	68
2	109	65	96	73
3	95	74	104	68
4	157	45		
5	77	91		
Mean±S.D. <sup>d</sup>	109 ± 30	68 ± 17	101 ± 5	70 ± 3

719 <sup>a</sup>Minus-strand synthesis is measured as the progression of reverse transcription between  
720 probe sites 3 and 6 (see FIG. 1B), a distance of 7,031 nucleotides (nt).

721 <sup>b</sup>Time course 1 for each cell type is shown in FIG. 2A; the other time courses for each  
722 cell type are independent experiments performed under identical conditions.

723 <sup>c</sup>Rates for minus-strand DNA synthesis were calculated as described in FIG. 2A.

724 <sup>d</sup>Standard deviation.

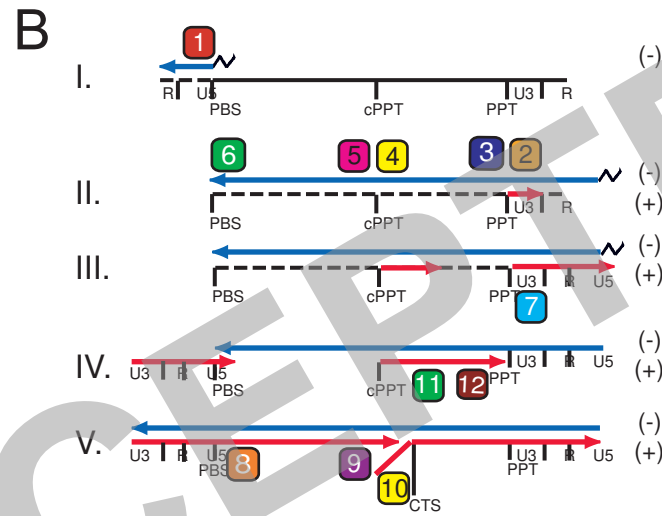
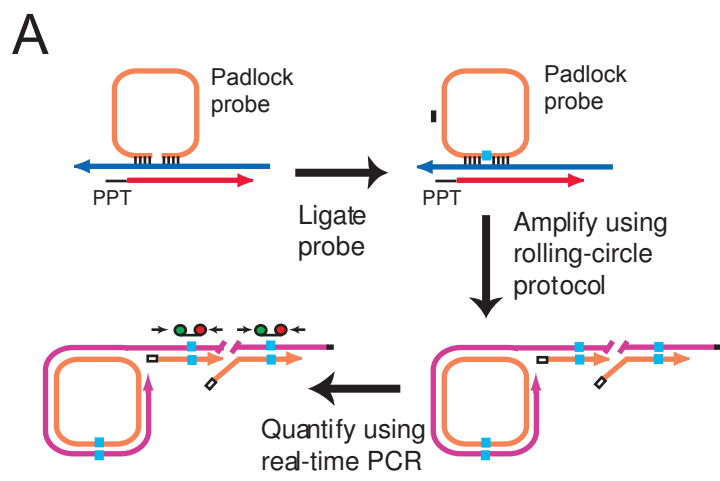
725 Table 5. Inhibition of HIV-1 replication with antiviral drugs.

Drug	Drug concentration	% Inhibition <sup>a</sup>
AZT	1 $\mu$ M	98.44 $\pm$ 1.16
ddI	50 $\mu$ M	97.46 $\pm$ 0.92
d4T	4 $\mu$ M	98.97 $\pm$ 0.18
EFV	9 nM	99.37 $\pm$ 0.05

726 <sup>a</sup> % Inhibition was calculated as 100% – % cells in drug treated samples that were  
727 positive for GFP expression, relative to the percentage of GFP-positive cells in the  
728 control infections in the absence of antiviral drugs. The percentage of GFP-positive cells  
729 was monitored by flow cytometry 36 h after infection. The results are shown as a mean  $\pm$   
730 standard deviation of two independent experiments.

731

ACCEPTED



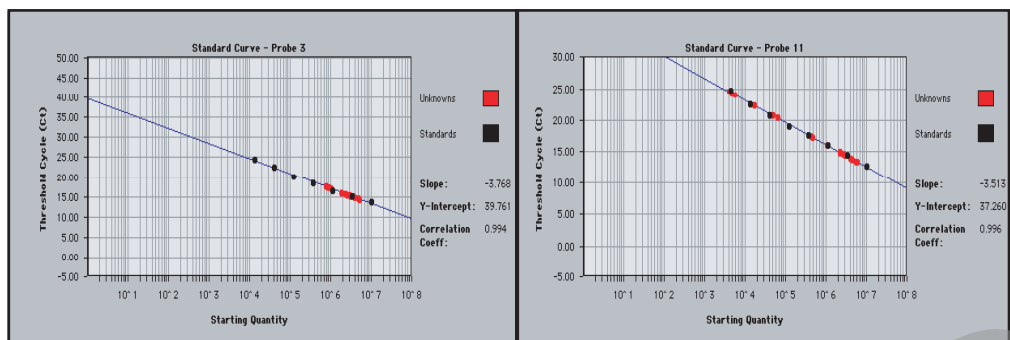
**C**

Spacer  
Ligation junction  
3' target arm  
5' target arm

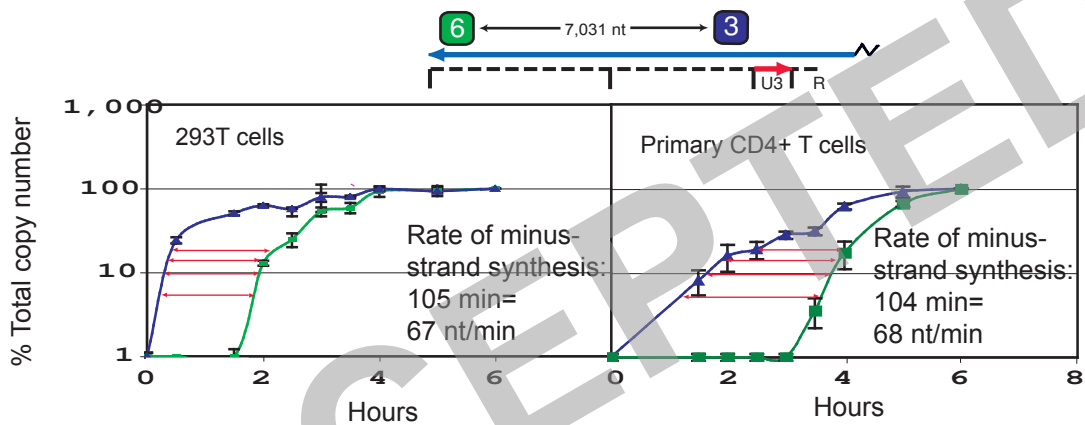
Probe	Spacer	Ligation junction	3' target arm	5' target arm
1	spacer-CCGTCTGTGTGTGAC/TCTGGTAACTAGAGATCC-spacer	F 579 T		
2	spacer-CCCTGATTGGCAGAAC/TACACACCCAGGGCCAGGG-spacer	F 7868 T		
3	spacer-CCTTTAAGACCAATGA/CTTACAAGGCAGCTGTAG-spacer	F 7728 T		
4	spacer-GTACAGTGCAGGGGAA/AGAATAGTAGACATAATA-spacer	F 4823 T		
5	spacer-GGCTGAACATCTTAAG/ACAGCAGTACAAATGGCA-spacer	F 4748 T		
6	spacer-TCTCTCGACGCAGGAC/TCGGCTTGCTGAAGCCGG-spacer	F 697 T		
7	spacer-CTGGCCCTGGTGTGTA/GTTCTGCCAATCAGGGAA-spacer	F 7868 T		
8	spacer-AAGCCGAGTCCTGCGT/CGAGAGATCTCCTCTGGC-spacer	F 688 T		
9	spacer-CCATTTGTACTGCTGT/CTTAAGATGTTACGCCTG-spacer	F 4748 T		
10	spacer-TATTATGTCTACTATT/CTTCCCCTGCACTGTAC-spacer	F 4825 T		
11	spacer-TTCACCTTTCAGAGG/AGCTTTGCTGGTCCTTTC-spacer	F 4951 T		
12	spacer-ATTGGTCTTAAAGGTA/CCTGAGGTGTGACTGGAA-spacer	F 7710 T		

Figure 1

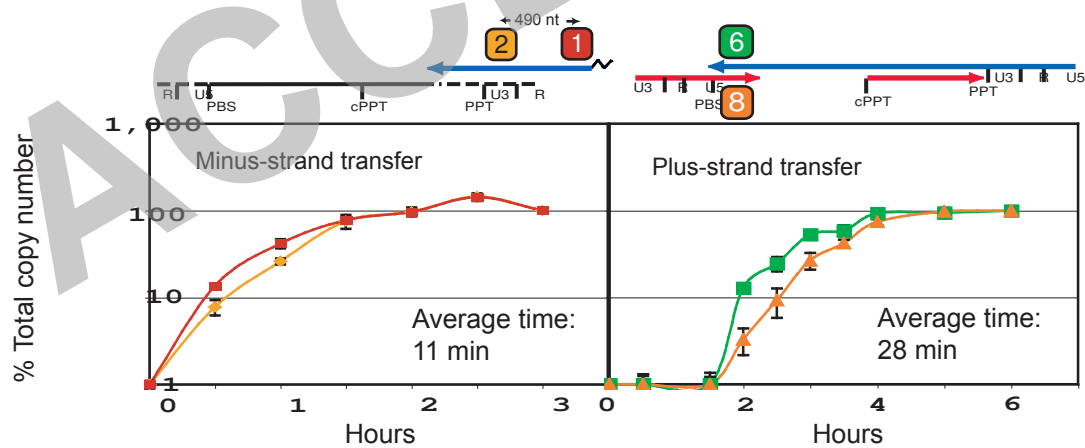
A



B



C



D

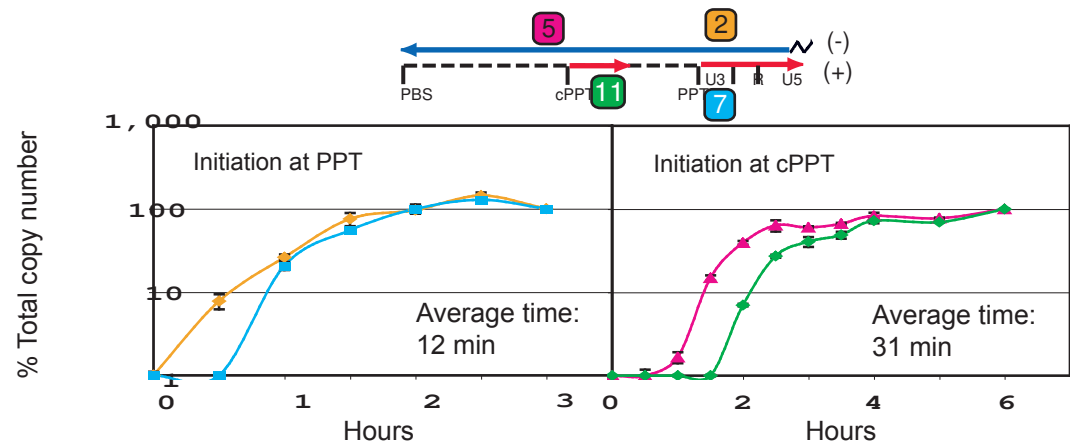


Figure 2

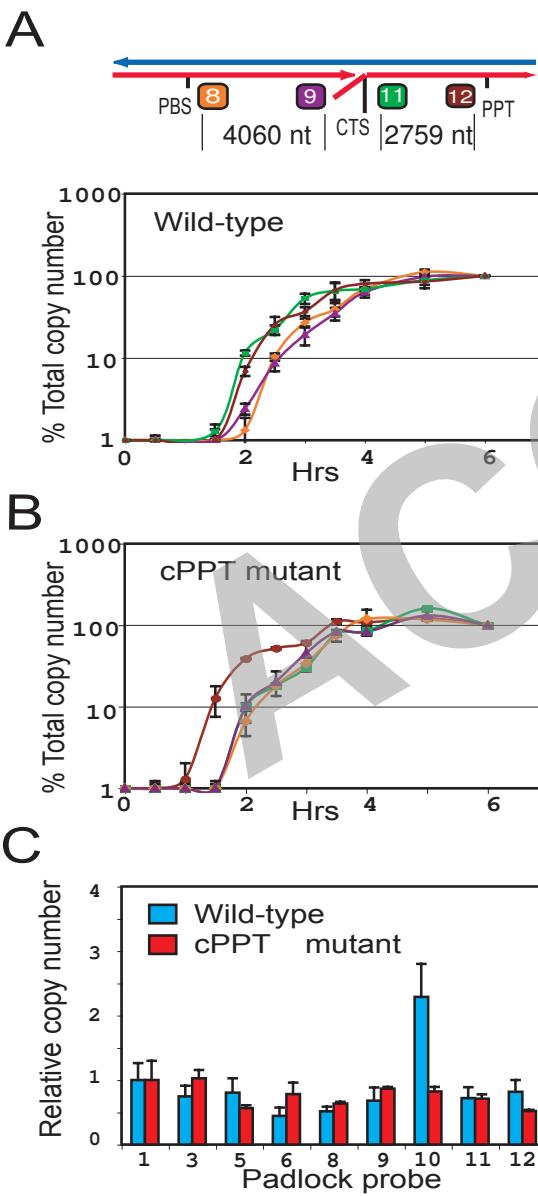


Figure 3

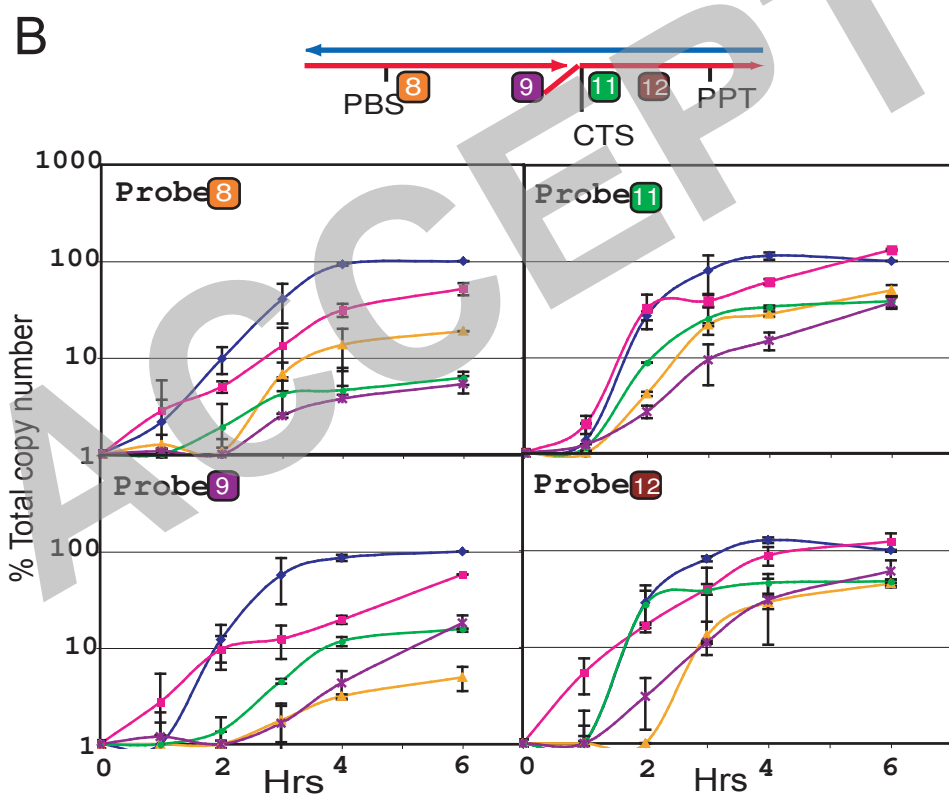
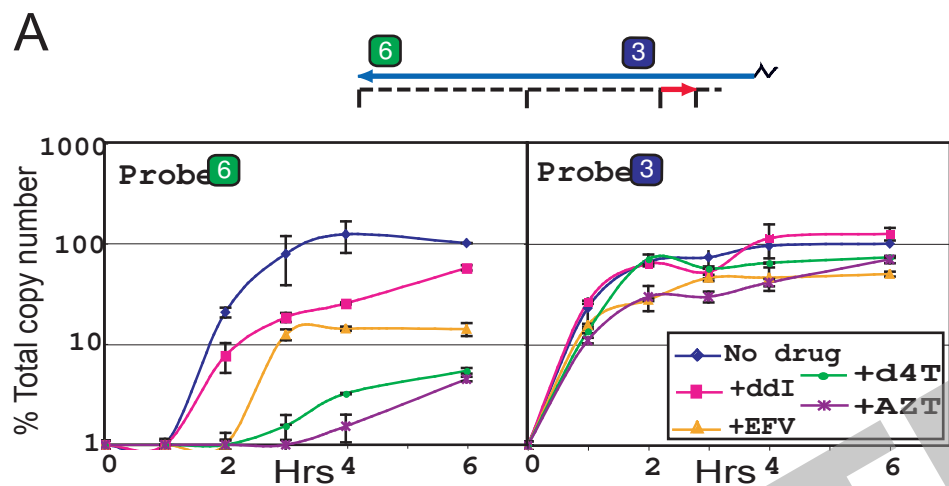


Figure 4